Crystal chemistry of brannockite, $KLi_3Sn_2Si_{12}O_{30}$, from a new occurrence in the Golden Horn Batholith, Washington State, USA

Markus B. RASCHKE, Evan J. D. ANDERSON, Julien ALLAZ, Henrik FRIIS, Joseph R. SMYTH, Rudy TSCHERNICH and Randy BECKER

Supplement

Microprobe analysis

Natural and synthetic standards are used for the EMP analysis: zircon from C.M. Taylor (Zr), SnO_2 (Sn), Hf metal (Hf), Amelia albite (Na, Si), anorthite USNM #137041 (Ca, Al), microcline USNM #143966 (K), fayalite USNM #85276 (Fe), ilmenite USNM #96189 (Ti), garnet P-130 (Mn), and Springwater olivine USNM #2566 (Mg). Background positions were chosen to avoid interferences. Counting time was optimized to improve detection limit (20 sec. on major elements, 30 seconds on Na, 40 seconds on Sn and Fe, 60 seconds on Al, Zr, Ti and Hf).

Micro-Raman analysis

An upright microscope (Olympus BH51) was used with a 632 nm HeNe laser excitation at 1 mW, 50x objective of NA = 0.8 and an imaging spectrograph (Princeton Instruments spectrometer Acton SP500, with PIXIS 100 liquid nitrogen cooled CCD camera, calibrated on multiple lines using a He-lamp).

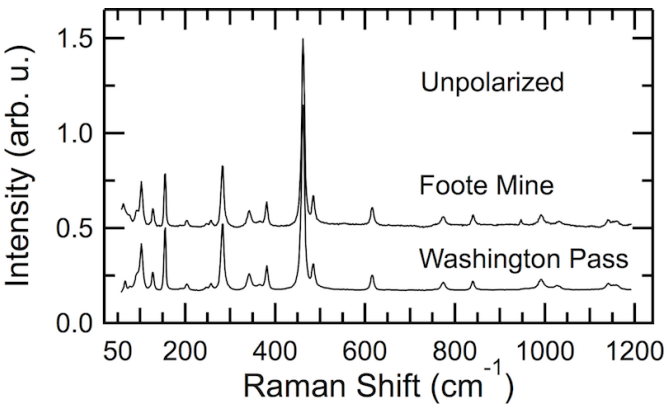

Fig. S1. Unpolarized micro-Raman spectra of brannockite from Foote Mine and Liberty Bell/Washington Pass.

Figure S1 shows unpolarized Raman spectra for both the Foote Mine and Washington Pass brannockite. The four most intense Raman peaks are 102.5 cm^{-1}, 155.6 cm^{-1}, 282.1 cm^{-1}, and 461.7 cm^{-1}, and are most likely associated with Si-O and Li-O phonon modes with dominance of the Si-O bending vibrations over the Si-O stretch vibrations. No resonances were found above 1200 cm^{-1}, indicating the absence of H_2O or bound OH-groups. The spectra are nearly identical in peak positions and line width with negligible background indicating high structural integrity of the crystals from both localities. Polarized Raman spectra and their anisotropy demonstrate the hexagonal crystal symmetry.

Figures S2 and S3 show additional polarization dependent Raman spectra. They exhibit a polarization anisotropy indicative of the hexagonal crystal symmetry. Light is incident either along or perpendicular with respect to the crystallographic *c*-axis, with H and V denoting combinations of the horizontal or vertical polarization of incident and detected light, respectively. H or V in figure S3 (a) and (b) alone represent the polarization of incident light, with unpolarized Raman detection. In figure S3 (a), the laser is incident parallel to the *c*-axis. In (b), the laser is incident perpendicular to the *c*-axis.

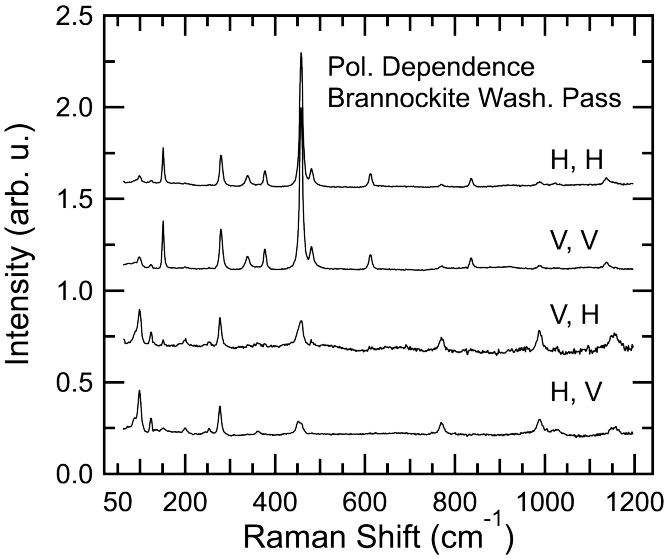

Fig. S2. Polarization dependence of prominent Raman peaks for Washington Pass brannockite. Data were taken on the crystal in Figure 2 (a) (main text). The HH, HV etc. combinations refer to the polarization of incident and detected light, respectively, with respect to the orientation of the sample as seen in Figure 2 (a).

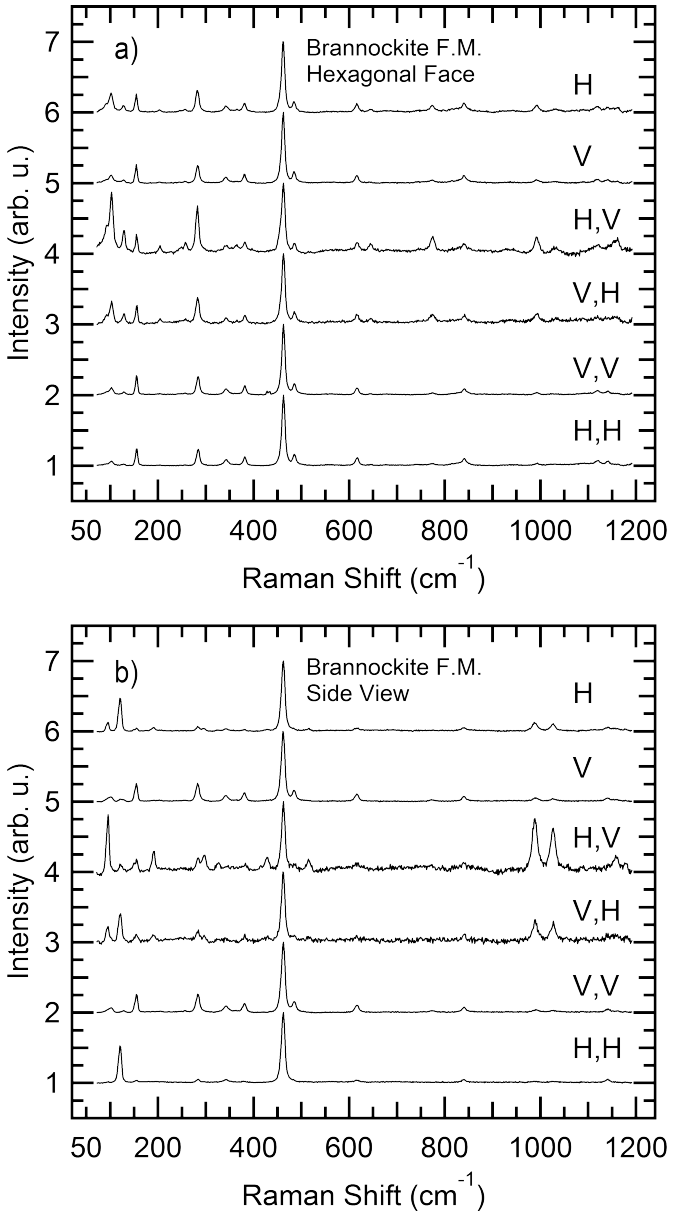

Fig. S3. Polarization dependence of prominent Raman peaks for Foote Mine brannockite. (a) shows data from the hexagonal face of the crystal, whereas (b) shows polarization dependence of the same crystal but on edge.

Structure refinement

The unit cell parameters were refined from centering angles of 60 strong reflections with 2ϑ between 10 and 28º using a point detector system on a Bruker P4 diffractometer. Intensity data were measured using a Bruker APEX II CCD detector. In all 29808 intensities were measured of which 978 were unique.

Similar to Foote Mine brannockite (Armbruster & Oberhänsli, 1988b), the Washington Pass crystals are twinned perpendicular to the (0001) plane. Crystal #4 showed significant amounts of the second twin member. Systematic absence violations of type 0,7, *l; l* – odd were observed, but could be resolved with the TWIN command in SHELXTL interchanging the *a*-axes.

To explore the occupancy of the main cation sites, their occupancies were released one by one. In the end, the A, B, C, and T1 sites were refined with their positions fixed. The T2, O1, O2, and O3 positions were free while their occupancies were fixed. When all atoms were located, they were made anisotropic. Using atomic scattering factors the data refined to R = 0.0336 for crystal #1 and 0.0359 for #4. These relatively high R_{int}-values (main text Table 4) are likely caused by a combination of the twinning and the compositional zoning. Similarly, the high R-values from Armbruster & Oberhänsli are associated with irregular crystal shape and resulting insufficient empirical absorption correction (Armbruster & Oberhänsli, 1988b).

The large T2 tetrahedron (Li-O: 1.93 Å) shows strong angular distortion as a result of the small but regular A octahedron (main text Fig. 3). This large irregular T2 tetrahedron is distinct from, e.g., milarite with smaller yet regular T2 tetrahedra occupied by Be. There the connected A octahedron with Ca is large and compressed along the c-axis (Armbruster & Oberhänsli, 1988b).

Site occupancies

The C site scattering (Table 5, main text) is in agreement with the ideal 1 K^+ occupancy, confirming that the possibly slight K^+ excess detected in EMP is residing on some different lattice sites, most likely the B vacancy site. Some excess scattering might be present for the T2 site compared to the ideal occupation with 3 Li^+ considering overestimation of site occupancy using atomic vs. ionic scattering factors for low Z elements. This excess in charge density on T2 could be due to Na^+ substitution, which is present in excess according to EMP analysis. While this assignment is speculative, we note that, e.g., in the mineral odintsovite $K_2Na_4Ca_3Ti_2Be_4Si_{12}O_{38}$, Na^+ and Li^+ were reported to share a similar disordered tetrahedral site (Rastsvetaeva *et al.* 1995). The assignment of Na^+ to T2, however, would not be compatible with the coupled substitution reaction discussed above which requires occupancy of a vacant site with the excess amount of Na^+ to achieve charge balance. Be^{2+} could be a possible Li^+ substituent. It could not only account for the excess charge but it would be consistent with the coupled substitution in the form: $^{A}(X^{4+}) + {}^{T2}Li^{+} \Leftrightarrow {}^{A}(Fe^{3+}, Al^{3+}) + {}^{T2}Be^{2+}$. Gadolinite found in the same cavity as brannockite confirms the general presence of Be^{2+}. However, a Be analysis could not be performed.

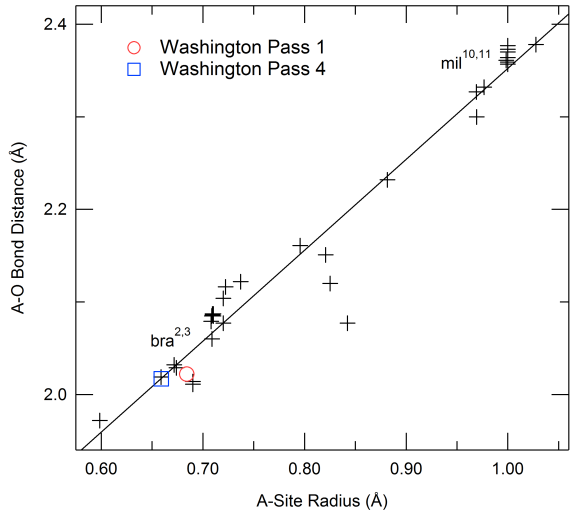

Fig. S4. <A-O> vs. A radius <r_A>, a good linear fit can be seen with $R^2 = 0.956$. Brannockite and Milarite are marked with brannockite data from this study (crystal 1 marked as a red circle and crystal 4 a blue square), and Armbruster & Oberhänsli, (1988b). Milarite data was obtained from Hawthorne *et al.*(1991) & Cerny *et al.*(1980).

Additional references cited*

Rastsvetaeva, R.K., Evsyunin, V.G., & Kashaev, A.A. (1995): Crystal structure of a new natural K,Na,Ca-titanoberyllosilicate. *Crystallography Reports*, **40**, 228-232.

*For other references see main text.

Table S1. Fractional coordinates and displacement parameters for Washington Pass brannockite using neutral scattering factors in comparison to data from Foote Mine (Armbruster & Oberhänsli 1988b). B_{eq} was converted from the Foote Mine values to Ueq using a conversion factor of $8\pi^2$. The B site is at 1/3, 2/3, 0 according to the P6/mcc space group. Armbruster reports it at 1/2, 2/3, 0, although correctly defines its position in the crystal structure diagram.

	Crystal 1x	Crystal 4	Armbruster 1		Crystal 1x	Crystal 4	Armbruster 1
C	(K)			O1			
x	0	0	0	x	0.1317(3)	0.1317(3)	0.1318(3)
y	0	0	0	y	0.3977(3)	0.3977(3)	0.3977(4)
z	1/4	1/4	1/4	z	0	0	0
Ueq	0.0197(7)	0.0177(6)	0.0180(3)	Ueq	0.0166(5)	0.0171(5)	0.0144(1)
U11	0.0184(8)	0.0164(7)	0.0157(5)	U11	0.023(1)	0.024(1)	0.019(1)
U22	0.0184(8)	0.0164(7)	0.0157	U22	0.019(1)	0.021(1)	0.016(1)
U33	0.023(1)	0.0202(9)	0.00174(8)	U33	0.006(1)	0.0069(9)	0.003(1)
U23	0	0		U23	0	0	
U13	0	0		U13	0	0	
U12	0.0092(4)	0.0082(3)	0.0079	U12	0.010(1)	0.012(1)	0.008(1)
A	(Sn)			O2			
x	1/3	1/3	1/3	x	0.2222(2)	0.2221(2)	0.2237(2)
y	2/3	2/3	2/3	y	0.2793(2)	0.2793(2)	0.2807(2)
z	1/4	1/4	1/4	z	0.1348(1)	0.1349(1)	0.1342(2)
Ueq	0.0058(2)	0.0061(1)	0.00503(4)	Ueq	0.0142(4)	0.0148(3)	0.0122(4)
U11	0.0054(2)	0.0057(1)	0.0046(1)	U11	0.0136(8)	0.0136(7)	0.0087(7)
U22	0.0054(2)	0.057(1)	0.0046	U22	0.0163(8)	0.0164(8)	0.0128(8)
U33	0.0066(2)	0.0067(2)	0.0045(1)	U33	0.0178(8)	0.0191(8)	0.0134(8)
U23	0	0		U23	0.0000(6)	-0.0005(6)	0.0004(6)
U13	0	0		U13	0.0001(6)	0.0008(6)	0.0006(6)
U12	0.00270(9)	0.0029(1)	0.0023	U12	0.0112(7)	0.0111(7)	0.0081(7)
T2	(Li)			O3			
x	1/2	1/2	1/2	x	0.1595(2)	0.1595(2)	0.1598(2)
y	1/2	1/2	1/2	y	0.5035(2)	0.5037(2)	0.1598(2)
z	1/4	1/4	1/4	z	0.1722(1)	0.1722(1)	0.1726(1)
Ueq	0.016(3)	0.013(2)	0.016(2)	Ueq	0.0108(4)	0.0108(3)	0.0074(2)
U11	0.021(4)	0.019(4)	0.019(4)	U11	0.0103(8)	0.0102(7)	0.0077(6)
U22	0.004(4)	0.008(4)	0.019	U22	0.0103(7)	0.0100(6)	0.0050(6)
U33	0.016(4)	0.009(4)	0.008(3)	U33	0.0111(8)	0.0113(7)	0.0072(6)
U23	0	0		U23	-0.0038(6)	-0.0040(5)	-0.0036(5)
U13	0	0		U13	-0.0021(6)	-0.0021(5)	-0.0013(5)
U12	0.002(2)	0.004(2)	0.015(4)	U12	0.0046(6)	0.0044(6)	0.0033(5)
T1	(Si)			B	(Na)		
x	0.23849(7)	0.23844(7)	0.23866(7)	x	1/3	1/3	
y	0.35614(7)	0.35620(7)	0.35649(7)	y	2/3	2/3	
z	0.39033(4)	0.39029(4)	0.39057(5)	z	0	0	
Ueq	0.0074(2)	0.0076(1)	0.0040(5)	U11	0.02	0.02	
U11	0.0074(3)	0.0079(3)	0.0038(2)				
U22	0.0078(3)	0.0080(3)	0.0041(2)				
U33	0.0071(3)	0.0070(3)	0.0029(2)				
U23	0.0010(2)	0.0008(2)	0.0022(2)				
U13	0.0006(2)	0.0006(2)	0.0006(2)				
U12	0.0039(2)	0.0040(2)	0.0011(2)				

Table S2. Fractional coordinates and displacement parameters for Washington Pass using ionic scattering factors. The Na in crystal 4 had a negative occupancy during refinement and was removed.

	Crystal 1x	Crystal 4		Crystal 1x	Crystal 4
C	(K)		O1		
x	0	0	x	0.1317(3)	0.1317(3)
y	0	0	y	0.3973(4)	0.3973(4)
z	1/4	1/4	z	0	0
Ueq	0.0195(7)	0.0178(6)	Ueq	0.0158(6)	0.0162(5)
U11	0.0183(8)	0.0167(7)	U11	0.022(1)	0.023(1)
U22	0.0183(8)	0.0167(7)	U22	0.018(1)	0.019(1)
U33	0.022(1)	0.0200(10)	U33	0.006(1)	0.008(1)
U23	0	0	U23	0	0
U13	0	0	U13	0	0
U12	0.0091(4)	0.0083(3)	U12	0.010(1)	0.011(1)
A	(Sn)		O2		
x	1/3	1/3	x	0.2222(2)	0.2222(2)
y	2/3	2/3	y	0.2794(2)	0.2794(2)
z	1/4	1/4	z	0.1346(1)	0.1345(1)
Ueq	0.0059(2)	0.0063(1)	Ueq	0.0135(4)	0.0139(4)
U11	0.0055(2)	0.0060(1)	U11	0.0130(8)	0.0127(8)
U22	0.0055(2)	0.0060(1)	U22	0.0156(9)	0.0156(8)
U33	0.0067(2)	0.0069(2)	U33	0.0167(9)	0.0182(8)
U23	0	0	U23	-0.0002(7)	-0.0007(7)
U13	0	0	U13	-0.0001(7)	0.0006(7)
U12	0.00277(9)	0.00300(7)	U12	0.0107(7)	0.0106(7)
T2	(Li)		O3		
x	1/2	1/2	x	0.1593(2)	0.1593(2)
y	1/2	1/2	y	0.5032(2)	0.5034(2)
z	1/4	1/4	z	0.1722(1)	0.1722(1)
Ueq	0.021(3)	0.020(3)	Ueq	0.0100(4)	0.0099(3)
U11	0.028(5)	0.028(4)	U11	0.0092(8)	0.0089(7)
U22	0.007(4)	0.013(4)	U22	0.0097(8)	0.0090(7)
U33	0.020(5)	0.014(4)	U33	0.0106(8)	0.0110(7)
U23	0	0	U23	-0.0036(6)	-0.0039(6)
U13	0	0	U13	-0.0022(6)	-0.0022(6)
U12	0.003(2)	0.007(2)	U12	0.0043(7)	0.0039(6)
T1	(Si)		B	(Na)	
x	0.23850(7)	0.23846(7)	x	1/3	
y	0.35617(8)	0.35623(7)	y	2/3	
z	0.39037(4)	0.39034(4)	z	0	
Ueq	0.0068(2)	0.0070(2)	U11	0.02	
U11	0.0069(3)	0.0073(3)			
U22	0.0072(3)	0.0074(3)			
U33	0.0064(3)	0.0063(3)			
U23	0.0009(2)	0.0008(2)			
U13	0.0006(2)	0.0006(2)			
U12	0.0036(2)	0.0037(2)			